Published in final edited form as:
Stem Cells. 2011 October ; 29(10): 1537–1548. doi:10.1002/stem.697.

Mesenchymal Stem Cells Expressing Insulin-like Growth Factor-I (MSC^{IGF}) Promote Fracture Healing and Restore New Bone Formation in Irs1 Knock-out Mice: Analyses of MSC^{IGF} Autocrine and Paracrine Regenerative Effects

Froilán Granero-Moltó[1], **Timothy J. Myers**[1], **Jared A. Weis**[1], **Lara Longobardi**[1], **Tieshi Li**[1], **Yun Yan**[1], **Natasha Case**[2], **Janet Rubin**[2], and **Anna Spagnoli**[1,3]

[1]Departments of Pediatrics, Division of Pediatric Endocrinology, University of North Carolina at Chapel Hill, Chapel Hill, North Carolina, USA

[2]Department of Internal Medicine, Division of Endocrinology, University of North Carolina at Chapel Hill, Chapel Hill, North Carolina, USA

[3]Department of Biomedical Engineering, University of North Carolina at Chapel Hill, Chapel Hill, North Carolina, USA

Abstract

Failures of fracture repair (non-unions) occur in 10% of all fractures. The use of mesenchymal stem cells (MSC) in tissue regeneration appears to be rationale, safe and feasible. The contributions of MSC to the reparative process can occur through autocrine as well as paracrine effects. The primary objective of this study is to find a novel mean, by transplanting primary cultures of bone marrow-derived MSC expressing insulin-like growth factor-I (MSC^{IGF}), to promote these seed-and-soil actions of MSC to fully implement their regenerative abilities in fracture repair and non-unions. MSC^{IGF} or traceable MSC^{IGF}-Lac-Z were transplanted into wild-type or insulin-receptor-substrate knock-out (*Irs1*$^{-/-}$) mice with a stabilized tibia fracture. Healing was assed using biomechanical testing, micro-computed-tomography (μCT) and histological analyses. We found that systemically transplanted MSC^{IGF} through autocrine and paracrine actions improved the fracture mechanical strength and increased new bone content while accelerating mineralization. We determined that IGF-I adapted the response of transplanted MSC^{IGF} to promote their differentiation into osteoblasts. *In vitro* and *in vivo* studies showed that IGF-I-induced induced osteoglastogenesis in MSC was dependent of an intact IRS1-PI3K

Address correspondence to: Anna Spagnoli M.D., Department of Pediatrics, Division of Pediatric Endocrinology, 103 Mason Farm Road, 3341 MBRB, Campus Box: 7039, University of North Carolina at Chapel Hill, Chapel Hill, North Carolina 27599-7039, USA. Phone: 919-843-6904; spagnoa@med.unc.edu.

Author contributions:
Froilán Granero-Moltó: Conception and design, collection and assembly of the data, data analysis and interpretation, manuscript writing.
Tim J. Myers: Collection and assembly of the data, data analysis and interpretation.
Jared A. Weis: Collection and assembly of the data, data analysis.
Lara Longobardi: Collection and assembly of the data, data analysis and interpretation.
Tieshi Li: Collection and assembly of the data, data analysis and interpretation.
Yun Yan: Collection and assembly of the data, data analysis and interpretation.
Natasha Case: Provision of study material.
Janet Rubin: Provision of study material.
Anna Spagnoli: Conception and design, financial support, administrative support, data analysis and interpretation, manuscript writing, final approval of the manuscript.

Disclosure of potential conflict of interest.
The authors indicate no potential conflicts of interest.

signaling. Furthermore, using *Irs1*$^{-/-}$ mice as a non-union fracture model through altered IGF signaling, we demonstrated that the autocrine effect of IGF-I on MSC restored the fracture new bone formation and promoted the occurrence of a well-organized callus that bridged the gap; a callus that basically absent in *Irs1*$^{-/-}$ left untransplanted or transplanted with MSC. We provided evidence of effects and mechanisms for transplanted MSC^{IGF} in fracture repair and potentially to treat non-unions.

Keywords

Mesenchymal stem cells; Fracture healing; Insulin-like growth factor; mouse models

Introduction

Nearly 10–20% of all fractures have impaired healing, including delayed unions and non-unions [1]. Impaired fracture healing, which requires prolonged or repeated treatments, has a marked impact on both the quality of life and the total cost of care. Several compounds and strategies aimed at enhancing fracture healing when non-unions or delayed unions occur are currently under investigation [2]. In recent years, special attention has been paid to adult mesenchymal stem cells (MSC), also known as mesenchymal stromal cells, due to their potential role in tissue regeneration. Initially, their multilineage differentiation potential (autocrine effect) generated the most interest, but more recently, their ability to define and manipulate the environment through supply and release of bioactives molecules (paracrine properties) is drawing the attention [3–7]. Understanding the autocrine and paracrine regenerative actions of MSC is a critical goal in adult stem cell regenerative medicine that will allow us to more effectively manipulate these cells for tissue repair. MSC can be isolated from bone marrow (BM) and other adult tissues [8]. We, and others, have demonstrated that MSC can differentiate into mature mesenchymal cell types and localize to the injured site in fracture mice improving the healing following systemic delivery [7, 9]. In addition, MSC can regulate the regenerative response in bone and other tissues by the secretion of trophic factors [3]. In several *in vivo* models of injury, where MSC have been shown to improve function and repair, variable levels of MSC engraftment and tissue-specific cell differentiation have been found [7, 10–13]. It is plausible that to fully empower the MSC differentiative capacity *in vivo*, cells need to be engineered with specific growth factors that would drive them into a defined lineage commitment, specifically into osteogenesis.

Insulin-like growth factor-I (IGF-I) is a potent anabolic growth factor. IGF-I activity is mediated by the IGF type 1 receptor (IGF1R) a ligand-dependent tyrosine kinase receptor. The binding of lGF-I to the IGF1R activates the autophosphorylation of its cytoplasmic kinase domain which through interaction with various docking proteins, including the insulin-receptor-substrate-1 IRS-1 and Src homology/α-collagen (SHC), activates downstream signaling pathways [14]. The two main signaling activated by IGF1R are the Ras/Raf/MAPK pathway [15, 16] and the phosphatidylinositol 3-kinase (PI3K)/AKT pathway [17, 18].

IGF-I has a central role in the growth and development of different tissues in the embryo [19]. Mice lacking *Igf1* and *Igf1r* exhibit delayed embryonic skeletal growth and bone mineralization together with retarded skeletal development [20, 21]. In accordance, targeted overexpression of IGF-I in osteoblasts enhanced bone growth and mineralization [22]. IGF-I also has an important role in post natal bone maintenance and post natal bone mass. In inbred strains of mice, levels of circulating IGF-I and bone mineral density (BMD) correlate [23]. In humans, circulating IGF-I and BMD correlate with incidence of fracture [24].

IGF-I administration accelerates fracture healing in different animal models [25–27]. In women with hip fracture, systemic administration of IGF-I along with IGFBP-3 improved healing, albeit modestly, and serum IGF-I levels were positively associated with a shorter time of healing [28, 29].

Numerous *in vitro* studies have documented the ability of the PI3K-AKT signaling to promote osteoblast differentiation [30, 31]. In *Irs1* knock-out mice $Irs1^{-/-}$ fractures fail to heal indicating that IRS-1 has a role in bone repair that cannot be compensated by other IGF signaling pathways or IRS isoforms [32, 33].

In this study we analyzed the role of the combined effects of MSC and IGF-I in bone regeneration using a model of tibia fracture and dissected the autocrine and paracrine contributions to the repair process. We found that systemically transplanted MSC expressing desIGF-I (MSC^{IGF}) improved the biomechanical properties of the fracture callus by increasing the callus strength, modulus of elasticity and toughness. We showed that the improvement of the biomechanical properties are related to a faster healing with an increase in bone content and earlier callus mineralization and accelerated expression of genes involved in bone repair. We were able to demonstrate by using Lac-Z cell tracking that within the fracture site, transplanted MSC^{IGF} differentiated into osteoblasts in a greater number than MSC. Most notably, we found that the autocrine properties of IGF-I expressed by MSC restored new bone fracture formation and partially rescued the lack of fracture healing found in $Irs1^{-/-}$ mice. Our studies provide evidence of a central role for MSC-derived IGF-I in bone regeneration, opening new applications to combined therapies of MSC and IGF-I to enhance bone repair in fracture non-unions.

Materials and Methods

Antibodies and Radioimmunossay (RIA)

Primary antibodies used were: phospho-$IRS1^{S307}$; podoplanin/E11 (Santa-Cruz-Biotechnology); alkaline phosphatase (ALP) (Abcam); osteocalcin (OCN) (TAKARA); IRS1 (Millipore); pan-AKT, phospho-AKT^{S473}, phospho-p44/42 $(ERK1/2)^{T202/Y204}$, ERK1/2 (Cell Signaling) and Actin (Sigma). Dmp1 antibody was provided by Dr. Chunlin Qin (Baylor College of Dentistry) [34]. Horseradish peroxidase conjugated anti-rabbit IgG and anti-mouse IgG secondary antibodies were from GE Healthcare. IGF-I was measured by RIA (DSL-Inc) that we verified to measure human IGF-I but that does not cross-react with mouse IGF-I.

Stabilized fracture model

All animal protocols were approved by the animal care committee of the University of North Carolina-Chapel Hill and Vanderbilt University. Stabilized tibia fractures were produced in 8–12 weeks old FVB female syngenic mice (FVB-NJ, Jackson-Laboratories), $Irs1^{-/-}$ and control mice in C57BL/6 background as previously described [7, 35].

DNA constructs

Human des(1–3) IGF-I (desIGF) was overexpressed in MSC using a retroviral vector. Human des(1–3) IGF-IA construct was obtained by directed mutagenesis of full length human IGF-IA isoform. The three first amino acids of the mature peptide (GPE) were removed from the full length cDNA of IGF-IA, inserted in a pBluescript vector using QuickChange-Site-Directed mutagenesis kit (Stratagene) using the primers: DesIGFI-F, 5'-ACCAGCTCTGCCACGGCTACGCTCTGCGGGGCTGAG-3' and DesIGFI-R, 5'-CTCAGCCCCGCAGAGCGTAGCCGTGGCAGAGCTGGT-3' according to the manufacturer's instructions. After mutagenesis, the des(1–3)IGF-IA isoform was released

from pBluescript backbone and inserted into the retroviral vector pMSCVpuro-EGFP to produce pMSCVpuro-desIGFI-EGFP.

Retroviral production

Retroviral supernatants of human des(1–3)IGF-I, *Irs1* shRNA and control vectors were produced in Phoenix Amphotrophic packaging cells (ATCC#SD 3443). pMSCVpuro vector containing des(1–3)IGF-IA cDNA, pRFP-C-RS containing small hairpin RNA against mouse *Irs1* mRNA (OriGene Technologies), pRFP-C-RS vector containing non-effective 29-mer scramble shRNA or pMSCVpuro-EGFP empty vector were transfected using Lipofectamine 2000 or Lipofectamine LTX (Invitrogen) according to the manufacturer's instructions. Sixteen hours after transfection the medium was replaced and the viral supernatants were harvest at 24 and 48 hours.

Isolation, expansion and retroviral infection of primary MSC

Primary cultures of BM-MSC were obtained by flushing the BM from femurs and tibias of 4–6 weeks old mice as previously reported [36]. BM nucleated cells were expanded for 3 days. At day 4, retroviral supernatants were added to the BM nucleated adhering cells with 4 μg/ml of freshly prepared hexadimethrine bromide (Sigma). The retroviral infection was repeated the following day. After 24-hour recovery the infected cells were selected for 3 days with the addition of 3 μg/ml of puromycin to the culture medium. MSC^{IGF} produced radio-immunoassayable levels of IGF-I in the conditioned medium (CM-MSC^{IGF}) and such IGF-I was bioactive as indicated by the fact that activated AKT phosphorylation when used to treat MSC (Fig. S1, A–B). Immediately before transplant into fractured mice, resistant colonies were immunodepleted of hematopoietic cells providing purified MSC expressing high levels of MSC markers as previously reported [7, 37]. After fracture, mice were transplanted with 10^6 MSC or MSC^{IGF} by tail vein injection. MSC were also isolated from the BM of $ROSA26^{CMV\text{-}Cre}$ mice and were transplanted into Lac-Z negative female littermates [7, 38]. The $ROSA26^{CMV\text{-}Cre}$ mice were generated by crossing the ROSA26R-LacZ mice (provided by Dr. Phil Soriano) with CMV-Cre mice as previously reported [7]. MSC were also obtained from C57BL/6 mice and transplanted into $Irs1^{-/-}$ mice (C57BL/6 background). Untransplanted littermates were used as control. The $Irs1^{-/-}$ mice homozygous for *Irs1* gene deletion were provided by Dr. C. R. Kahn [39].

Biomechanical testing (BMT) and micro-computedtomography (μCT) analysis of fracture calluses

Fractured tibias were dissected 14 days post-fracture and following removal of the pin, μCT-scanned (Scanco Medical μCT40) or subjected to BMT testing as previously described [7]. More details on the method used to determine the material callus types by μCT analyses are reported in Supplemental Methods.

Established MSC, culture conditions and in vitro osteoblastic differentiation

For *in vitro* experiments, a BM-derived MSC were derived from C57BL/6 wild type mice using the procedure of Peister *et al.* [40]. Cells were maintained in growth medium (αMEM supplemented with 10% fetal bovine serum. For differentiation experiments, cells were plated at a density of 5000 cells per cm^2 and expanded in growth medium for 3 days. Osteoblastic differentiation was induced in serum-free conditions in differentiation medium (αMEM supplemented with 50 μg/ml of ascorbic acid, 10 mM of β-glycerol phosphate). When indicated, human recombinant des(1–3)IGF-I (Gropep) was added to the differentiation medium at 100 ng/ml. Differentiation medium was changed every 3 days. Differentiation was assayed 14 days after induction by Alizarin Red staining. For Alizarin Red staining, after medium aspiration, MSC were washed with PBS, fixed in 70% ethanol

for 10 minutes at room temperature and stained for 15 min with a 2% solution of Alizarin Red. After staining, excess of Alizarin Red was washed out with distilled water and plates were photographed. Calcium deposits were solubilized incubating overnight the cells with 0.5 N HCl and quantified using a QuantiChrom-Calcium Assay Kit (BioAssay-Systems) according to the manufacturer's instructions. Calcium deposits were expressed as μM/well. For retroviral studies, MSC cultures were infected with the retroviral supernatants one day after plating at low density in the same conditions as the MSC used for *in vivo* studies. The infection was repeated the following day, and after one day recovery resistant colonies were selected using 2 μg/ml puromycin in the culture medium. The presence of puromycin was maintained during expansion and removed for differentiation purposes.

Western blotting

Whole cell lysates where prepared with lysis buffer (50 mM TrisHCl, 150 mM NaCl, 0.5% Triton X-100, 0.1% SDS, pH 7.4) supplemented with 50 mM NaF, 2 mM Na_3VO_4, 2 mM phenylmethylsulfonylfluoride. Ten-micrograms of protein-lysates were loaded in 10% SDS-polyacrilamide gels and transferred to polyvinylidene-fluoride membranes (Millipore). Membranes were blocked with 5% non-fat milk. Primary antibodies were incubated overnight at 4 °C. Bands were detected with secondary antibodies conjugated with HRP in combination with ECL enhanced chemiluminescence kit (GE Healthcare).

Histology Immunohistochemistry and in situ hybridization

Tibias, at least 3 per group, were dissected at 7, 10 and 14 days post-fracture, histologically prepared and the entire callus sectioned (6 μm). Safranin O/Fast Green staining was prepared as previously reported [7]. *In situ* hybridization analysis was performed as previously described [41]. Plasmids with cDNA insertion of mouse *Collagen 1a1* (*Col1*), *Osterix (Osx)* and *Osteocalcin* (Ocn) were provided by G. Karsenty (Columbia University). The probe for mouse *Collagen 10a1 (Col10a1)* has been previously described [41]. Immunohistochemistry was done using Vectastain ABC kit (Vector-Laboratories) according to the manufacturer's instructions. Images were taken using an Olympus1X71 microscope with a DP71 camera, imported into Adobe Photoshop and formatted without using any imaging enhancement. Quantifications of the *in situ* hybridization imaging were performed through the use of a custom-built image analysis code (MATLAB, MathWorks). See more details in Supplemental Methods.

X-Gal staining

X-Gal staining was performed as previously reported, using a protocol that did not result in any background in no cell transplantation control [742]. The percentage of Lac-Z positive cells over the number of Fast Red positive cells within the same size area of interest of the cortical bone adjacent to the fracture line was quantified in at least 2 bones per group at day 7 post fracture in at least 4 sections selected within the center of the fracture.

Cell migration assay

Cell migration was estimated using a modified Boyden chamber as described in the Supplemental Methods section.

Statistical analysis

Data are expressed as means ± SD. Multiple comparisons are analyzed by one-way ANOVA, followed by Bonferroni *ad-hoc* testing for all pairwise multiple comparisons, Single comparisons are analyzed by unpaired Student's *t*-test. The GraphPad 5.0 software was used. Statistical significance is set at $p<0.05$.

Results

MSC^{IGF} transplant improves fracture healing

The effects of MSC^{IGF} transplant in fracture repair were first investigated by BMT. Dissected tibias (14 days after fracture) from control fractured mice that did not received cell transplant (No cells), from mice that received MSC transplant (MSC) and mice that received MSC expressing des-IGF-I transplant (MSC^{IGF}) were subjected to distraction force to failure BMT. MSC^{IGF} induced stronger calluses as indicated by a significant increase in ultimate force over untransplanted controls and MSC transplanted mice (165% and 140% increase respectively) (Fig. 1A). MSC^{IGF} transplant induced distinct changes in the mechanical properties of the repairing callus. Mice that received MSC^{IGF} showed an increase of the modulus of elasticity compared to mice that received MSC alone or did not receive cells. (Fig. 1C). Mice that received MSC alone showed an increase of ultimate displacement compared to the mice that did not receive cells (Fig. 1B). Both MSC and MSC^{IGF} transplants significantly increased the toughness of the callus with respect to the untransplanted control group indicating the ability to absorb more energy before failure (Fig. 1D). The different responses in the biomechanical outputs (modulus of elasticity and ultimate displacement) indicate that MSC and MSC^{IGF} increase the callus toughness and therefore the resistance to fracture by different mechanisms, respectively making either a more ductile callus (MSC^{IGF}) or a more rubbery callus (MSC) and point to more new bone formation in calluses of MSC^{IGF} recipients. This observation led us to investigate the distinct changes in callus composition induced by IGF-I expression in MSC.

MSC^{IGF} transplant induces new bone formation in fractured calluses

To determine how IGF-I overexpression by MSC was affecting the tissue composition of the callus, dissected tibias from the three study groups were subjected to μCT analyses 14 days after fracture. After 3D reconstruction, the callus volumes as well as new bone volume contents and soft tissue contents were measured according to our previously reported μCT-histological based thresholding analysis summarized in Supplemental Methods [7]. MSC^{IGF} transplant distinctly determined a significant increase in the amount of new bone content in the callus (new bone) over MSC and untransplanted controls (Fig. 2A). We observed that MSC^{IGF} recipients consistently formed calluses that contained bone bridging the fracture gap. This bone continuity was minimal in the calluses from mice in the other groups (Fig. 2B, arrowheads). These findings are consistent with the BMT results indicating that recipients of MSC^{IGF} had stronger bones with increased modulus of elasticity and toughness due to more new bone formation.

To further characterize the components of the callus, we histologically analyzed the callus composition at different time points during fracture healing. Histological Safranin O/Fast Green staining analyses of sections obtained at the fracture line showed that 7 days post-fracture calluses from No cells, MSC and MSC^{IGF} transplanted mice had a similar morphological appearance, although the No cells group showed smaller calluses (Fig. 3A, 7 days). At day 10 post-fracture, MSC^{IGF} calluses showed remarkably different compositions compared to calluses from MSC and No cells recipients. MSC^{IGF} transplanted group showed a callus mostly composed of bone tissue (light green staining) (Fig. 3A, 10 days), while the MSC and No cells transplanted groups were characterized by the presence of abundant cartilage content at different stages of endochondral ossification (red staining) (Fig. 3A, 10 days). These differences persisted at 14 days (Fig. 3A, 10 days) and were particularly evident when coronal sections of calluses from MSC and MSC^{IGF} were compared (Fig S2, A). Interestingly, these differences in callus composition were unique to the fracture line with mostly new bone in MSC^{IGF} recipients and mostly soft tissue in MSC recipients, while no differences in bone and cartilage were detected when sections

proximally and distally outlying the fracture line were examined (Fig S2, B). To further evaluate the nature of the callus tissues, cross-sections of 10 and 14 days calluses were subjected to *in situ* hybridization analyses for cartilage and bone markers. At day 10 post-fracture, calluses from mice that received MSC^{IGF} transplant showed a prevalent expression of bone markers namely *Osx*, *Ocn* and *Col1* and reduced expression of the cartilage marker *Col10* compared with mice that received only MSC or to the No cells control group (Fig. 3B, and Fig. S3 for quantitative analysis). Similarly, at day 14 post-fracture, we observed that calluses from MSC^{IGF} recipients exhibited marginal expression of *Col10* and extended areas of bone marker expressions (*Osx*, *Ocn* and *Col1)*. While calluses from MSC transplant showed persistent areas of *Col10* expression and less expression of bone markers (Fig. 3C and Fig. S3 for quantitative analysis). Additionally, we observed that when compared with MSC transplanted recipients, calluses from mice that received MSC^{IGF} transplant were comprised of abundant areas of intramembranous ossification, especially at the fracture line (Fig. 4, arrowheads). Taken together, longitudinal histological and *in situ* analyses indicate that MSC^{IGF} transplant induces an acceleration of the callus mineralization mostly progressing through intramembranous ossification.

IGF-I induces MSC osteoblast differentiation in vivo: autocrine and paracrine effects

We have previously shown that systemically delivered MSC migrate to the bone fracture site where they home within the BM and in particular to the endosteum [7]. However, we noted that the number of transplanted MSC that differentiated into osteoblasts was low and mostly localized in the cortical bone close to the fracture site [7]. We investigated whether the expression of IGF-I in MSC induced commitment of transplanted MSC into bone cells. MSC were isolated from *ROSA26*$^{CMV\text{-}Cre}$ mice that constitutively express the bacterial β-galactosidase gene and were retrovirally infected to produce MSC^{IGF}-Lac-Z or MSC-Lac-Z. We tracked the localization of the transplanted cells by X-gal staining 7 days post-fracture and compared with MSC-Lac-Z transplanted animals. In MSC^{IGF}-Lac-Z recipients, we detected an abundant amount of Lac-Z positive cells in the cortical bone adjacent to the fracture line (27.5 ±6.0% Lac-Z positive cells over nuclear Fast Red positive cells counted in 4 regions of interest in 4 sections from 2 bones) while a minimal number of Lac-Z positive cells was found in the same region of interest in calluses from MSC-Lac-Z recipients (3.7±0.7%; n=4; p=0.0002 *vs* MSC^{IGF}-Lac-Z). MSC^{IGF}-Lac-Z engraftment was in addition to the localization of cells in the BM, along the endosteal surfaces in the fracture rim that was similar to what was seen in MSC-Lac-Z recipients (Fig. 5A, a and b). In addition, the MSC^{IGF}-Lac Z positive cells that integrated in the cortical bone morphologically resembled osteocytes and osteoblasts. The morphological appearance was confirmed by co-immunostaining of Lac-Z positive cells for Dmp I (that has been largely reported to be highly expressed by osteocytes) (Fig. 5A, e) and for the osteoblast marker Ocn (Fig. 5A, f) [43–47]. These findings indicate that *in vivo*, IGF-I induces fracture-engrafted MSC^{IGF} to differentiate into bone cells.

IGF-I has been reported to induce MSC migration and in C3H10T1/2 pluripotent cells Runx2 effects on migration are blocked by treatment with an IGF-I antibody [30, 48]. To investigate whether IGF-I secreted by MSC^{IGF} would be a chemotactic factor for MSC we examined cell migration in a chemotaxis assay. As shown in Fig. S4, we found that MSC^{IGF}–CM induced MSC migration while MSC-CM had no effect. MSC^{IGF}–CM effects on migration were similar to the potent chemo-attractant PGDF used as a positive control. Interestingly, when IGF-I was added to either the control medium or to MSC-CM did not induce cell migration. These results indicate that in MSC^{IGF} , IGF-I through an autocrine effect stimulates the secretion of a chemotactic factor that induces MSC migration.

We then evaluated whether IGF-I signaling was activated within the calluses of MSC^{IGF} through the detection of phsophorylated IRS1. An increased number of cells that were

positive for phospho-IRS1 (pIRS) was noted in calluses of MSC^{IGF}-Lac-Z recipients (Fig. 5B, d) compared to MSC-Lac-Z (Figure 5B, c). We also noted that to the increase of pIRS1-positive cells comprised MSC^{IGF}-Lac-Z (double positive for Lac-Z and pIRS1, brown dark), as well as host cells that were adjacent to Lac-Z-pIRS1 cells (pIRS1 positive but Lac-Z negative, light orange). Calluses from mice that received MSC^{IGF}-Lac-Z transplant showed in the same region where pIRS1 positive cells were found, high expressions for OCN (Fig. 5B, e–f), E11 (Fig. 5B, g–h) and ALP (Fig 5B, j–k) that are highly expressed by bone cells [49, 50]. As with the pIRS-1 positive cells, bone marker positive cells were either MSC^{IGF}-Lac-Z double positive or adjacents to MSC^{IGF}-Lac-Z. These findings indicate that MSC^{IGF} improve the fracture repair by promoting new bone formation through autocrine and paracrine mechanisms.

MSC osteogenic differentiation induced by IGF-I is mediated through the IRS1-PI3K pathway

We next sought to determine the intracellular mechanisms through which IGF-I promote MSC osteogenic through *in vitro* studies. MSC were induced to differentiate in osteogenic serum-free medium in the presence or absence of desIGF-I and with and without LY294002 (PI3K specific inhibitor) or U0126 (MEK specific inhibitor). The addition of desIGF-I induced MSC differentiation into osteoblasts as indicated by the increased mineralization detected by Alizarin Red staining and calcium deposits quantification (Fig. 6, A and B). Such process was impaired by the LY294002 but was insensitive to U0126 treatment (Fig. 6, A and B). At the concentrations used, both inhibitors efficiently blocked the transduction of the expected pathways, determined by the presence of the phosphorylated forms of AKT (PI3K pathway) and ERK1/2 (MEK pathway), without interfering with each other (Fig. S5). Furthermore, inhibitors did not affect cell viability as confirmed by the presence of a similar number of cells (by nuclei staining) after 14 days of treatment (Fig. 6A, lower panels).

To define the mechanism trough which IGF-I activates the PI3K pathway we silenced *Irs1* mRNA in MSC and assayed their ability to undergo osteogenic differentiation. We stably infected cells with retroviruses carrying an *Irs1* specific shRNA, *Irs1* silencing was confirmed by RT-PCR (Fig. 6C). Infected cells displayed reduced IRS1 phosphorylation after desIGF-I induction compared to the shRNA control cells. Blocking *Irs1* expression and activity caused a decrease in IGF-I dependent AKT phosphorylation, but had no effect on ERK 1/2 phosphorylation (Fig. 6D). In addition, *Irs1* silencing impaired osteoblastic differentiation of MSC as measured by Alizarin Red staining (Fig. 6E). Taken together these data indicate that IGF-I induces osteoblast differentiation of MSC through activation of the IRS1-PI3K pathway and independently of MAPK signaling.

In the $Irs1^{-/-}$ mouse model of fracture non-union, MSC^{IGF} transplant through an autocrine mechanism restores the new bone fracture formation and partially rescue the fracture healing

We decided to further dissect the role of the autocrine properties of IGF-I in transplanted MSC^{IGF}. IRS-1 has been reported to have a critical role in fracture healing as indicated by the fact $Irs1^{-/-}$ mice have fracture healing failure [32, 33]. We had demonstrated that *Irs1* was required for IGF-I mediated osteoblastic differentiation of MSC *in vitro*, therefore, we used the $Irs1^{-/-}$ mice with impaired IGF-I signaling in host cells to determine the autocrine IGF-I effects on transplanted MSC in a model of non-union fracture repair. At day 14 post-fracture, $Irs1^{-/-}$ mice showed almost absence of callus formation (Fig. S6, A–B). MSC^{IGF} transplant in $Irs1^{-/-}$ mice, evaluated 14 days after fracture, induced the formation of abundant new bone callus bridging the fracture line, callus that remained practically absent in $Irs1^{-/-}$ mice that were not transplanted or that received only MSC (Fig. 7A). When quantified, the amount of new bone at the fracture line in $Irs1^{-/-}$ recipients of MSC^{IGF} was

significantly higher (double) than the amount found in *Irs1*$^{-/-}$ untransplanted mice, while MSC transplant had no effect (Fig. 7B). Soft tissue was also significantly increased in MSC^{IGF} recipients while MSC alone had no effect (Fig. 7B). The amount of bone formed at the fracture line in *Irs1*$^{-/-}$ recipients of MSC^{IGF} became not significantly different than the amount found in wild-type mice while the soft tissue was still lower (Fig. S7). Histological analyses illustrated that calluses of MSC^{IGF} transplanted *Irs1*$^{-/-}$ mice had abundant bone and cartilage formation, while in untransplanted and MSC recipients the fracture line demonstrated an accumulation of cells that were negative for bone or cartilage markers and resembled fibroblastic tissue (Fig. 7C). In summary, the autocrine actions of IGF-I on transplanted MSC was sufficient to restore new bone formation in *Irs1*$^{-/-}$ mice and partially rescued (soft tissue is still lower than the one found in wild-type) their fracture repair process.

Discussion

In this study, we demonstrated that transplanted MSC^{IGF} accelerates the fracture healing process. We determined *in vivo*, that IGF-I promotes MSC commitment to differentiated bone cells and induce bone formation through paracrine and autocrine actions within the fracture. We identified the unique and essential role of the IRS1-PI3K pathway in mediating the IGF-I dependent osteogenic effects on MSC. Lastly, we found that MSC^{IGF} through the autocrine effects of IGF-I are sufficient to restore the fracture new bone formation and partially rescued the fracture healing process in a non-union mouse model with a defective IGF signaling.

Studies on MSC have been escalating over the past years due to their potential role in tissue regeneration: first because of their multilineage differentiation potential and more recently, to the characterization of their paracrine/trophic properties [3–6, 51]. It now appears evident that MSC function both as multipotent cells and as cells that provide the microenvironment for other progenitors. Therefore, MSC embody properties of both the “seed” and the “soil” for tissue regeneration. Understanding and empowering these properties will allow us to develop “intelligently-programmed MSC” that smoothly engraft into a damage tissue and promote repair. In the present study, we have demonstrated that augmenting MSC with IGF-I allow MSC to maximize the coupling of their differentiative and trophic activities. Attempts to use MSC in fracture repair in clinical and animal studies have shown some beneficial effects [52, 53]. The beneficial effects of IGF-I overexpression in MSC have been also reported in wound and tendon healing, in these healing models the paracrine actions of IGF-I mediated the beneficial effects [54, 55]. Although these studies have proved the concept that MSC can be beneficial, they have not provided evidences for the mechanisms underlying these effects. We found that MSC^{IGF} transplant accelerates the fracture repair process through transplanted MSC differentiation into bone cells and host cell differentiation (paracrine effect). We had seen an acceleration of the intramembranous mineralization process of the callus and resulting, restoration of biomechanical integrity of the bone. The discovery of a paracrine/trophic function of MSC and the fact that although MSC are beneficial, a low number of engrafted and terminally differentiated donor-MSC are found into the repaired tissue has led investigators to be inclined toward supporting the hypothesis that the paracrine/trophic function plays a more critical role in regeneration. Our study, demonstrates that the differentiative and therefore regenerative abilities of transplanted-MSC can be promoted *in vivo* with the aid of growth factors and has opened new prospective for the use of MSC-based therapy combined with IGF-I in fracture repair.

At the present, the clinical application of MSC retrovirally manipulated to express IGF-I is impracticable because the concerns of undesired immunological responses and the carcinogenic potential of the retroviral systems [56]. On the other hand, IGF-I therapy has

been shown to be safe and effective in treating children with growth hormone insensitivity that leads to IGF-I deficiency. The present study provides fundamental data for developing combined MSC and IGF-I therapies to promote fracture repair. We envision a clinical use of MSC similar to the one employed in BM transplant in which hematopoietic stem cell therapy is combined with growth factor therapy to promote hematopoiesis.

The effects of MSC^{IGF} on promoting differentiation of transplanted MSC into bone cells can be either autocrine or due to the effects of secreted IGF-I on recipient cells (i.e. local MSC or other cell types) that then signal to the transplanted MSC. To explore one of these potential effects, we evaluated the chemotactic action of CM from MSC^{IGF} on MSC migration. Although we found that CM-MSC^{IGF} induced MSC migration, this effect was not due directly to the secreted IGF-I but to a secretory factor that was induced by IGF-I acting on MSC^{IGF} through an autocrine mechanism, as indicated by the fact that added IGF-I was ineffective. Other effects of secreted IGF-I on other recipient cells that could have induced transplanted MSC^{IGF} differentiation cannot be excluded and these as well as the identification of this IGF-I-induced chemotactic factor would be the objectives of future investigations.

On the other hand, to further investigate the autocrine effects of IGF-I on transplanted MSC, we have used a genetic approach by transplanting MSC^{IGF} into *Irs1*$^{-/-}$ recipients that lack the IGF-I signaling and therefore the IGF-paracrine response and have fracture healing failure. We found that MSC^{IGF} could rescue the callus new bone formation and partially the soft tissue of *Irs1*$^{-/-}$ recipients, providing a clear evidence for IGF-I autocrine effects on transplanted MSC^{IGF}. Most of the animal models for non-unions are based on large osteotomies or periosteal removal. The lack of healing in these models is due to multiple complex factors. This complexity makes the assessment of the potential beneficial effects of therapeutic interventions difficult at best. Our studies in a mouse model of non-union due to a knock-out of a specific gene (*Irs1*) has provided the first evidence that MSC transplant can rescue a failure in fracture healing by providing expression of a specific growth factor that promotes new bone formation.

Numerous *in vitro* studies have documented the ability of IGF-I and IRS-PI3K-AKT signaling to promote osteoblastic differentiation [31, 57–60]. In our study, we have confirmed the essential role of the IRS1 signaling in the commitment of MSC into bone cells *in vitro* and extended this finding to *in vivo* by showing that: 1) MSC differentiated into bone cells within the callus also show an activated IRS-1 signal and 2) in mice lacking the IRS-1 signaling the autocrine effects of IGF-I are capable of promoting fracture repair.

Summary

In summary, our studies provide evidence that transplanted MSC^{IGF}: 1) promote the fracture repairing process by accelerating the callus mineralization; 2) engraft and integrate into the callus differentiating into bone cells; 3) control and interact with the fracture repairing environment of the recipients promoting trophic effects; 3) exert their autocrine osteogenic functions through the IRS-1 signaling; 4) rescue the new bone fracture healing in a monogenic model of non-union, namely Irs1$^{-/-}$ mice. The information generated by our studies provides the fundamental theoretical and mechanistic bases for the development of MSC/IGF-I clinical trials in patients with non-unions.

Supplementary Material

Refer to Web version on PubMed Central for supplementary material.

Acknowledgments

This work was supported by NIH-NIDDK, grant number R01DK070929-06 to A. Spagnoli. We acknowledge the equipment support of the UNC-Biomedical Research Imaging Center for the μCT imaging; Dr. Michael Miga (Vanderbilt University) for some of the BMT measurements and Dr. Chunlin Qin (Baylor College of Dentistry) for the Dmp1 antibody. Dr. C. Ronald Kahn (Joslin Diabetes Center, Boston) for the *Irs1*$^{-/-}$ mice.

References

1. Praemer, AF.; S; Rice, DP. Musculoskeletal Conditions in the United States Rosemont, Illinois. 1999.
2. Axelrad TW, Kakar S, Einhorn TA. New technologies for the enhancement of skeletal repair. Injury. 2007; 38(Suppl 1):S49–S62. [PubMed: 17383486]
3. da Silva Meirelles L, Caplan AI, Nardi NB. In search of the in vivo identity of mesenchymal stem cells. Stem cells (Dayton, Ohio). 2008; 26:2287–2299.
4. Nauta AJ, Fibbe WE. Immunomodulatory properties of mesenchymal stromal cells. Blood. 2007; 110:3499–3506. [PubMed: 17664353]
5. Caplan AI. Adult mesenchymal stem cells for tissue engineering versus regenerative medicine. Journal of cellular physiology. 2007; 213:341–347. [PubMed: 17620285]
6. Bianco P, Robey PG, Simmons PJ. Mesenchymal stem cells: revisiting history, concepts, and assays. Cell stem cell. 2008; 2:313–319. [PubMed: 18397751]
7. Granero-Molto F, Weis JA, Miga MI, et al. Regenerative effects of transplanted mesenchymal stem cells in fracture healing. Stem Cells. 2009; 27:1887–1898. [PubMed: 19544445]
8. da Silva Meirelles L, Chagastelles PC, Nardi NB. Mesenchymal stem cells reside in virtually all post-natal organs and tissues. J Cell Sci. 2006; 119:2204–2213. [PubMed: 16684817]
9. Granero-Molto F, Weis JA, Longobardi L, et al. Role of mesenchymal stem cells in regenerative medicine: application to bone and cartilage repair. Expert Opin Biol Ther. 2008; 8:255–268. [PubMed: 18294098]
10. Gandia C, Arminan A, Garcia-Verdugo JM, et al. Human dental pulp stem cells improve left ventricular function, induce angiogenesis, and reduce infarct size in rats with acute myocardial infarction. Stem Cells. 2008; 26:638–645. [PubMed: 18079433]
11. Ortiz LA, Dutreil M, Fattman C, et al. Interleukin 1 receptor antagonist mediates the antiinflammatory and antifibrotic effect of mesenchymal stem cells during lung injury. Proc Natl Acad Sci U S A. 2007; 104:11002–11007. [PubMed: 17569781]
12. Togel F, Weiss K, Yang Y, et al. Vasculotropic, paracrine actions of infused mesenchymal stem cells are important to the recovery from acute kidney injury. Am J Physiol Renal Physiol. 2007; 292:F1626–F1635. [PubMed: 17213465]
13. Iso Y, Spees JL, Serrano C, et al. Multipotent human stromal cells improve cardiac function after myocardial infarction in mice without long-term engraftment. Biochem Biophys Res Commun. 2007; 354:700–706. [PubMed: 17257581]
14. Kato H, Faria TN, Stannard B, et al. Role of tyrosine kinase activity in signal transduction by the insulin-like growth factor-I (IGF-I) receptor. Characterization of kinase-deficient IGF-I receptors and the action of an IGF-I-mimetic antibody (alpha IR-3). J Biol Chem. 1993; 268:2655–2661. [PubMed: 7679099]
15. Rozakis-Adcock M, McGlade J, Mbamalu G, et al. Association of the Shc and Grb2/Sem5 SH2-containing proteins is implicated in activation of the Ras pathway by tyrosine kinases. Nature. 1992; 360:689–692. [PubMed: 1465135]
16. Baltensperger K, Kozma LM, Cherniack AD, et al. Binding of the Ras activator son of sevenless to insulin receptor substrate-1 signaling complexes. Science. 1993; 260:1950–1952. [PubMed: 8391166]
17. Myers MG Jr, Backer JM, Sun XJ, et al. IRS-1 activates phosphatidylinositol 3'-kinase by associating with src homology 2 domains of p85. Proc Natl Acad Sci U S A. 1992; 89:10350–10354. [PubMed: 1332046]
18. Pelicci G, Lanfrancone L, Grignani F, et al. A novel transforming protein (SHC) with an SH2 domain is implicated in mitogenic signal transduction. Cell. 1992; 70:93–104. [PubMed: 1623525]

19. Powell-Braxton L, Hollingshead P, Warburton C, et al. IGF-I is required for normal embryonic growth in mice. Genes Dev. 1993; 7:2609–2617. [PubMed: 8276243]
20. Liu JP, Baker J, Perkins AS, et al. Mice carrying null mutations of the genes encoding insulin-like growth factor I (Igf-1) and type 1 IGF receptor (Igf1r). Cell. 1993; 75:59–72. [PubMed: 8402901]
21. Wang Y, Nishida S, Sakata T, et al. Insulin-like growth factor-I is essential for embryonic bone development. Endocrinology. 2006; 147:4753–4761. [PubMed: 16857753]
22. Zhao G, Monier-Faugere MC, Langub MC, et al. Targeted overexpression of insulin-like growth factor I to osteoblasts of transgenic mice: increased trabecular bone volume without increased osteoblast proliferation. Endocrinology. 2000; 141:2674–2682. [PubMed: 10875273]
23. Rosen CJ, Dimai HP, Vereault D, et al. Circulating and skeletal insulin-like growth factor-I (IGF-I) concentrations in two inbred strains of mice with different bone mineral densities. Bone. 1997; 21:217–223. [PubMed: 9276086]
24. Langlois JA, Rosen CJ, Visser M, et al. Association between insulin-like growth factor I and bone mineral density in older women and men: the Framingham Heart Study. J Clin Endocrinol Metab. 1998; 83:4257–4262. [PubMed: 9851760]
25. Raschke M, Wildemann B, Inden P, et al. Insulin-like growth factor-1 and transforming growth factor-beta1 accelerates osteotomy healing using polylactide-coated implants as a delivery system: a biomechanical and histological study in minipigs. Bone. 2002; 30:144–151. [PubMed: 11792577]
26. Schmidmaier G, Wildemann B, Heeger J, et al. Improvement of fracture healing by systemic administration of growth hormone and local application of insulin-like growth factor-1 and transforming growth factor-beta1. Bone. 2002; 31:165–172. [PubMed: 12110430]
27. Fowlkes JL, Thrailkill KM, Liu L, et al. Effects of systemic and local administration of recombinant human IGF-I (rhIGF-I) on de novo bone formation in an aged mouse model. J Bone Miner Res. 2006; 21:1359–1366. [PubMed: 16939394]
28. Boonen S, Rosen C, Bouillon R, et al. Musculoskeletal effects of the recombinant human IGF-I/IGF binding protein-3 complex in osteoporotic patients with proximal femoral fracture: a double-blind, placebo-controlled pilot study. J Clin Endocrinol Metab. 2002; 87:1593–1599. [PubMed: 11932288]
29. Di Monaco M, Vallero F, Di Monaco R, et al. Serum levels of insulin-like growth factor-I are positively associated with functional outcome after hip fracture in elderly women. American journal of physical medicine & rehabilitation / Association of Academic Physiatrists. 2009; 88:119–125.
30. Fujita T, Azuma Y, Fukuyama R, et al. Runx2 induces osteoblast and chondrocyte differentiation and enhances their migration by coupling with PI3K-Akt signaling. J Cell Biol. 2004; 166:85–95. [PubMed: 15226309]
31. Mukherjee A, Rotwein P. Akt promotes BMP2-mediated osteoblast differentiation and bone development. J Cell Sci. 2009; 122:716–726. [PubMed: 19208758]
32. Ogata N, Chikazu D, Kubota N, et al. Insulin receptor substrate-1 in osteoblast is indispensable for maintaining bone turnover. J Clin Invest. 2000; 105:935–943. [PubMed: 10749573]
33. Shimoaka T, Kamekura S, Chikuda H, et al. Impairment of bone healing by insulin receptor substrate-1 deficiency. J Biol Chem. 2004; 279:15314–15322. [PubMed: 14736890]
34. Baba O, Qin C, Brunn JC, et al. Colocalization of dentin matrix protein 1 and dentin sialoprotein at late stages of rat molar development. Matrix Biol. 2004; 23:371–379. [PubMed: 15533758]
35. Bonnarens F, Einhorn TA. Production of a standard closed fracture in laboratory animal bone. J Orthop Res. 1984; 2:97–101. [PubMed: 6491805]
36. Spagnoli A, Longobardi L, O'Rear L. Cartilage disorders: potential therapeutic use of mesenchymal stem cells. Endocr Dev. 2005; 9:17–30. [PubMed: 15879685]
37. Longobardi L, Granero-Molto F, O'Rear L, et al. Subcellular localization of IRS-1 in IGF-I-mediated chondrogenic proliferation, differentiation and hypertrophy of bone marrow mesenchymal stem cells. Growth Factors. 2009; 27:309–320. [PubMed: 19639489]
38. Soriano P. Generalized lacZ expression with the ROSA26 Cre reporter strain. Nat Genet. 1999; 21:70–71. [PubMed: 9916792]

39. Araki E, Lipes MA, Patti ME, et al. Alternative pathway of insulin signalling in mice with targeted disruption of the IRS-1 gene. Nature. 1994; 372:186–190. [PubMed: 7526222]
40. Peister A, Mellad JA, Larson BL, et al. Adult stem cells from bone marrow (MSCs) isolated from different strains of inbred mice vary in surface epitopes, rates of proliferation, and differentiation potential. Blood. 2004; 103:1662–1668. [PubMed: 14592819]
41. Spagnoli A, O'Rear L, Chandler RL, et al. TGF-beta signaling is essential for joint morphogenesis. J Cell Biol. 2007; 177:1105–1117. [PubMed: 17576802]
42. Chandler RL, Chandler KJ, McFarland KA, et al. Bmp2 transcription in osteoblast progenitors is regulated by a distant 3' enhancer located 156.3 kilobases from the promoter. Molecular and cellular biology. 2007; 27:2934–2951. [PubMed: 17283059]
43. Hauschka PV, Lian JB, Cole DE, et al. Osteocalcin and matrix Gla protein: vitamin K-dependent proteins in bone. Physiol Rev. 1989; 69:990–1047. [PubMed: 2664828]
44. Lee NK, Sowa H, Hinoi E, et al. Endocrine regulation of energy metabolism by the skeleton. Cell. 2007; 130:456–469. [PubMed: 17693256]
45. Kyono A, Avishai N, Ouyang Z, et al. FGF and ERK signaling coordinately regulate mineralization-related genes and play essential roles in osteocyte differentiation. Journal of bone and mineral metabolism. 2011
46. Kamiya N, Takagi M. Differential expression of dentin matrix protein 1, type I collagen and osteocalcin genes in rat developing mandibular bone. Histochem J. 2001; 33:545–552. [PubMed: 12005026]
47. Feng JQ, Huang H, Lu Y, et al. The Dentin matrix protein 1 (Dmp1) is specifically expressed in mineralized, but not soft, tissues during development. J Dent Res. 2003; 82:776–780. [PubMed: 14514755]
48. Fiedler J, Brill C, Blum WF, et al. IGF-I and IGF-II stimulate directed cell migration of bone-marrow-derived human mesenchymal progenitor cells. Biochemical and biophysical research communications. 2006; 345:1177–1183. [PubMed: 16716263]
49. Wetterwald A, Hoffstetter W, Cecchini MG, et al. Characterization and cloning of the E11 antigen, a marker expressed by rat osteoblasts and osteocytes. Bone. 1996; 18:125–132. [PubMed: 8833206]
50. Hadjiargyrou M, Rightmire EP, Ando T, et al. The E11 osteoblastic lineage marker is differentially expressed during fracture healing. Bone. 2001; 29:149–154. [PubMed: 11502476]
51. Keating A. Mesenchymal stromal cells. Current opinion in hematology. 2006; 13:419–425. [PubMed: 17053453]
52. Hauzeur JP, Gangji V. Phases 1–3 clinical trials using adult stem cells in osteonecrosis and nonunion fractures. Stem Cells Int. 2010:410170. [PubMed: 21048847]
53. Crovace A, Favia A, Lacitignola L, et al. Use of autologous bone marrow mononuclear cells and cultured bone marrow stromal cells in dogs with orthopaedic lesions. Vet Res Commun. 2008; 32(Suppl 1):S39–S44. [PubMed: 18688750]
54. Schnabel LV, Lynch ME, van der Meulen MC, et al. Mesenchymal stem cells and insulin-like growth factor-I gene-enhanced mesenchymal stem cells improve structural aspects of healing in equine flexor digitorum superficialis tendons. J Orthop Res. 2009; 27:1392–1398. [PubMed: 19350658]
55. Chen L, Tredget EE, Wu PY, et al. Paracrine factors of mesenchymal stem cells recruit macrophages and endothelial lineage cells and enhance wound healing. PLoS One. 2008; 3:e1886. [PubMed: 18382669]
56. Myers TJ, Granero-Molto F, Longobardi L, et al. Mesenchymal stem cells at the intersection of cell and gene therapy. Expert Opin Biol Ther. 10:1663–1679. [PubMed: 21058931]
57. Giustina A, Mazziotti G, Canalis E. Growth hormone, insulin-like growth factors, and the skeleton. Endocr Rev. 2008; 29:535–559. [PubMed: 18436706]
58. McCarthy TL, Centrella M, Canalis E. Regulatory effects of insulin-like growth factors I and II on bone collagen synthesis in rat calvarial cultures. Endocrinology. 1989; 124:301–309. [PubMed: 2909370]

59. Thomas T, Gori F, Spelsberg TC, et al. Response of bipotential human marrow stromal cells to insulin-like growth factors: effect on binding protein production, proliferation, and commitment to osteoblasts and adipocytes. Endocrinology. 1999; 140:5036–5044. [PubMed: 10537129]

60. Mukherjee A, Wilson EM, Rotwein P. Selective signaling by Akt2 promotes bone morphogenetic protein 2-mediated osteoblast differentiation. Molecular and cellular biology. 30:1018–1027. [PubMed: 19995912]

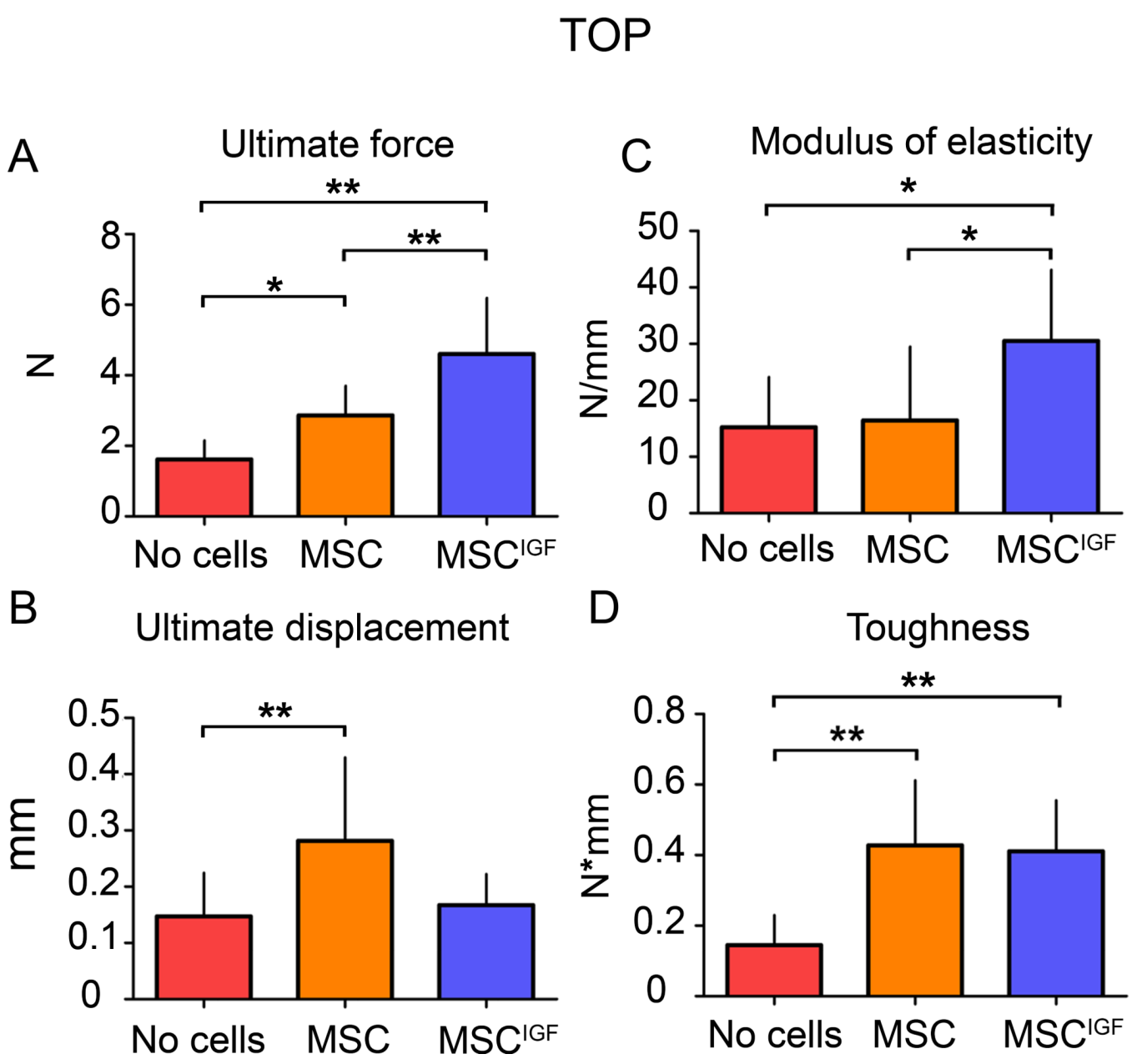

Figure 1.

Transplanted MSC^{IGF} improve the callus biomechanical properties differently from MSC. Fourteen days after tibia fracture, calluses from mice that had received either MSC or MSC^{IGF} transplant after the fracture or remained untransplanted (No cells) were dissected and subjected to distraction to failure BMT. p values of one-way ANOVA analyses are respectively: p=0.0001 for ultimate force; p=0.02 for ultimate displacement; p=0.02 for modulus of elasticity; p=0.0002 for toughness. *, p<0.05, **, p<0.01 by Bonferroni *post hoc* test. No cells, n=11, MSC, n=10, MSC^{IGF}, n=5.

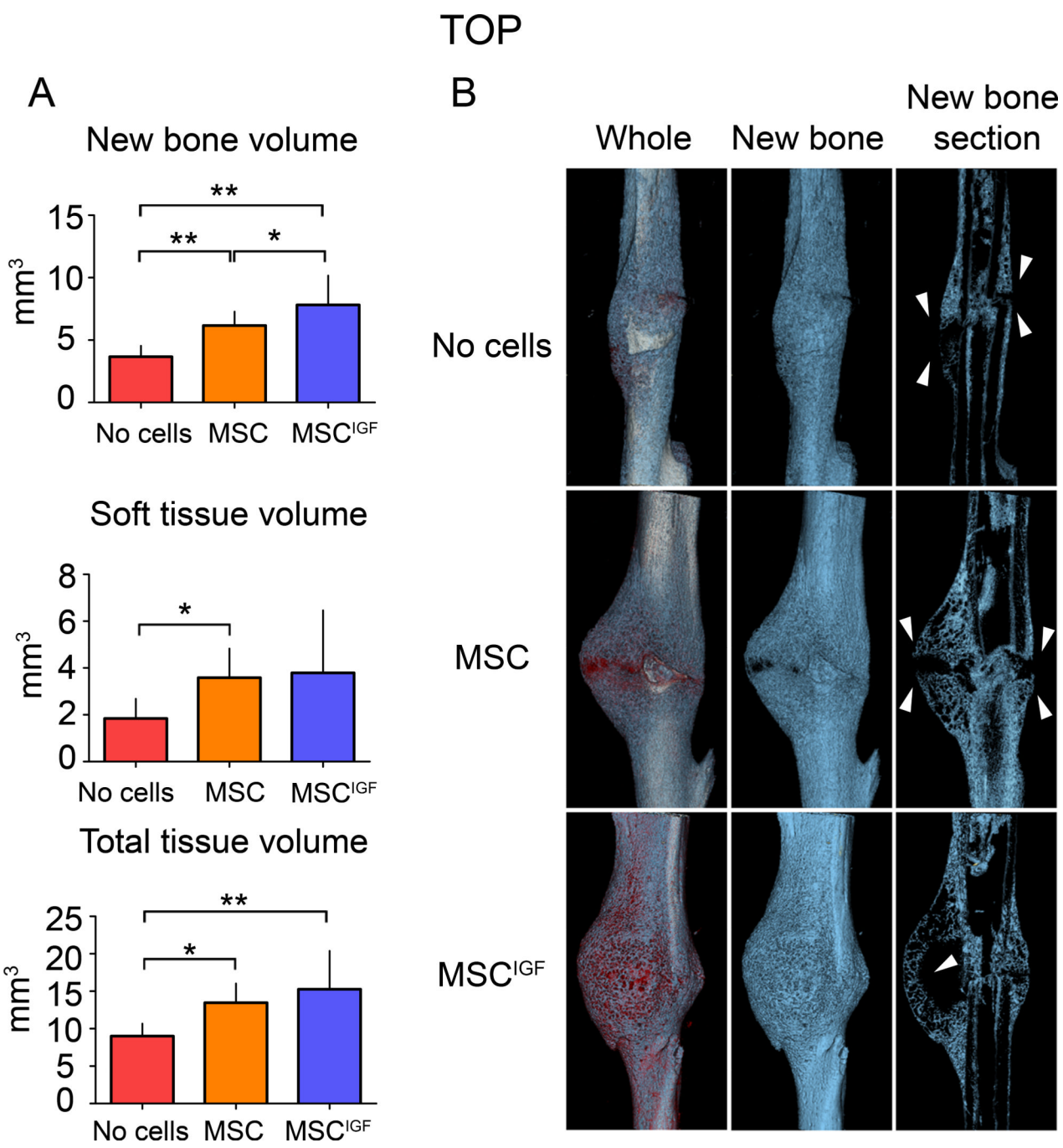

Figure 2.

MSC^{IGF} transplant increases the fracture callus new bone content. μCT analyses were performed on 14 day post-fracture tibias in transplanted mice (either with MSC or MSC^{IGF}) and untransplanted mice (No cells). **A,** total tissue volume, new bone volume (blue) and soft tissue volume (red) were calculated as reported in the Supplemental Methods section. New bone volume, ANOVA p-value=0.0006; soft tissue, ANOVA p-value=0.0395; total tissue volume, ANOVA p-value=0.0058. *, p<0.05; **, p<0.01 by Bonferroni *post hoc* test.. No cells, n=7; MSC, n=10; MSC^{IGF}, n=7. **B,** Three dimensional reconstruction of representative calluses from control (No cells) and MSC transplanted mice (MSC, MSC^{IGF}).

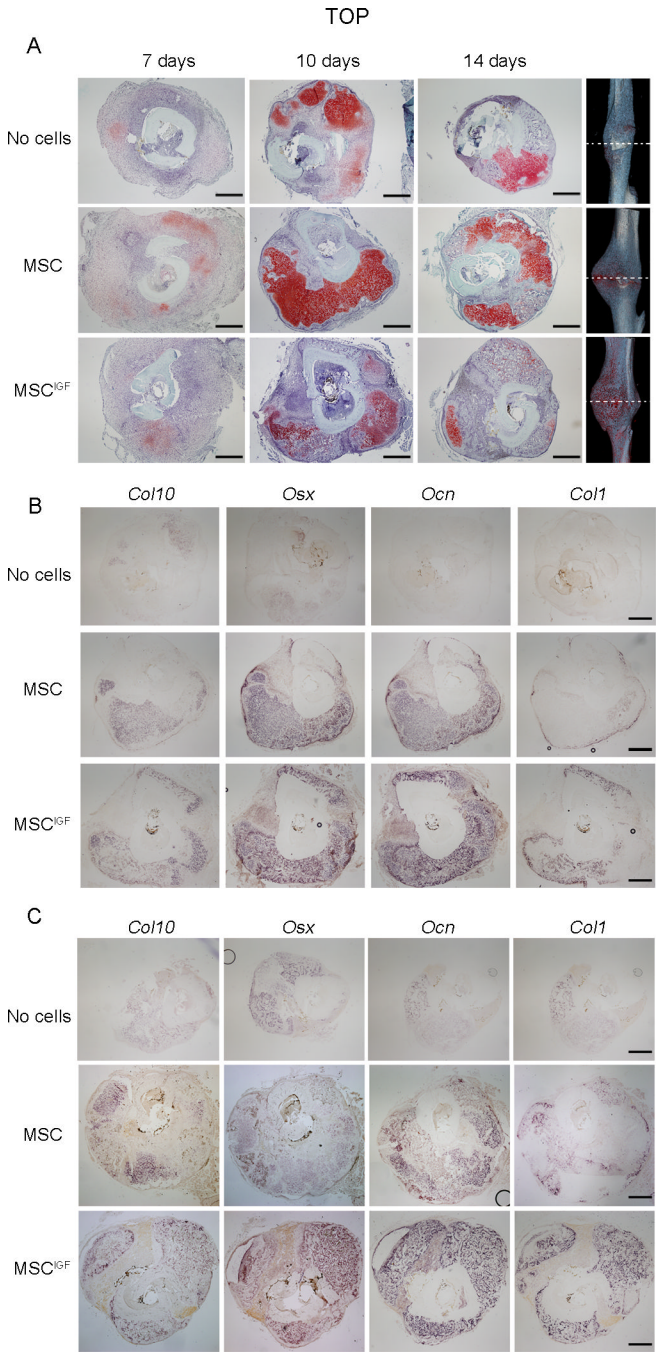

Figure 3.

MSC^{IGF} transplant induces bone formation that bridges the fracture gap. Histological sections were obtained from calluses of either MSC or MSC^{IGF} recipients or from mice that were left in transplanted (No cells) respectively 7, 10 and 14 days after fracture. **A,** Serial cross-sections of 7, 10 and 14 days fracture calluses were visualized with Safranin O/Fast Green staining for the presence of cartilage (red) and bone (green), depicted are sections of the fracture line. Ten (**B**) and fourteen (**C**) days post fracture calluses were analyzed by *in situ* hybridization for the presence of bone and cartilage markers namely *Col10*, *Osx*, *Ocn* and *Col1*. Bar, 500 μm.

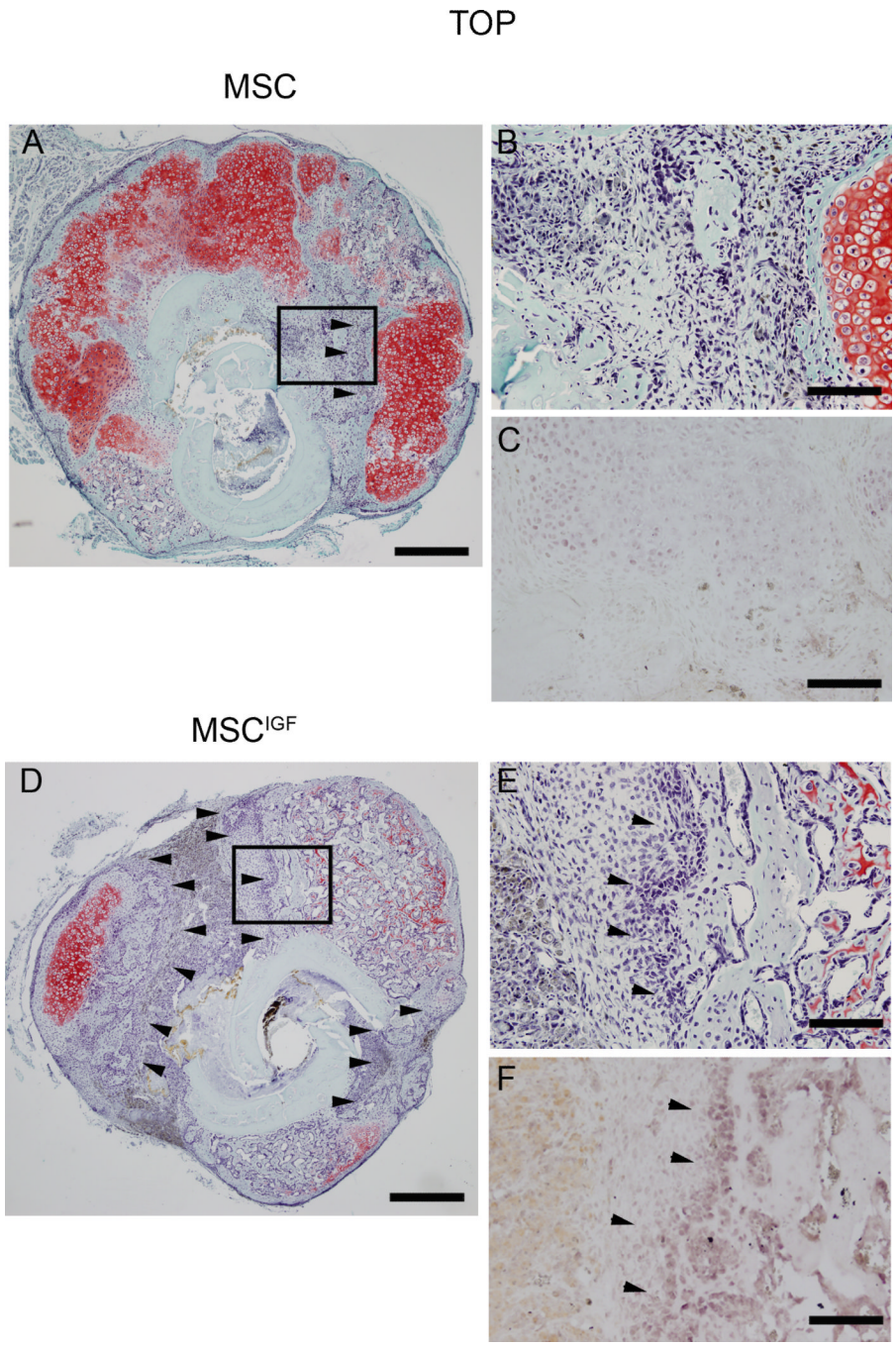

Figure 4.
MSC^{IGF} transplant increases the areas of intramembraneous ossification. Serial cross-sections of 14 days post-fracture calluses from mice either transplanted with MSC (**A,B,C**) or MSC^{IGF} (**D,E,F**) were subjected to Safranin O/Fast Green staining to visualize the presence of cartilage (red) and bone (green). In MSC^{IGF} recipients the Fast Green stainable areas of intramembraneous ossification were also positive for *Osx* detected by *in situ* hybridization (C, F) (arrowheads). Bar, 500 μm (A,D). 100 μm (B,C,E,F).

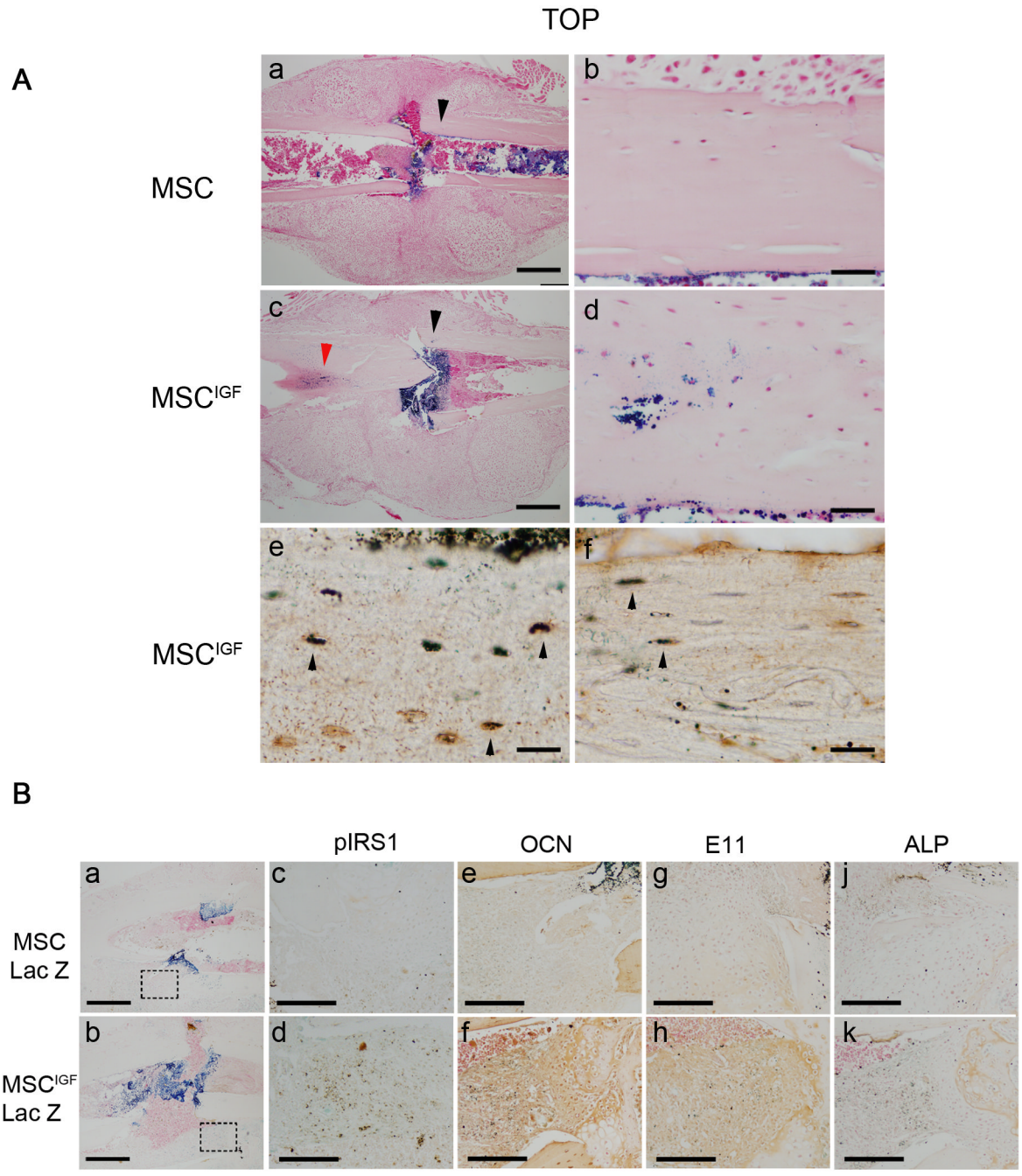

Figure 5.

IGF-I induces MSC osteoblastic differentiation *in vivo* through autocrine and paracrine mechanisms. Mice were transplanted with either MSC-Lac-Z or MSC^{IGF}–Lac-Z. Calluses were obtained 7 days after fracture and subjected to Lac-Z staining. **A**, (a), MSC-Lac-Z positive cells localize within the calluses at the endosteum, bone marrow and fracture rim. (c), in addition to these locations, MSC^{IGF}-Lac-Z positive cells localize in the cortical bone (arrow heads). (d), magnification of the area indicated by the black arrow head in (c). (e), histological sections from MSC^{IGF}–Lac-Z recipients adjacent to the section depicted in (a), were subjected to IHC for DMP-1 following Lac-Z staining. DMP-1-Lac-Z double positive

cells are depicted as dark brown cells (indicated by arrow-heads); DMP1 single positive in orange; Lac-Z single positive (none in this section) as light blue. (f), histological sections from MSC^{IGF}–Lac-Z recipients adjacent to the section depicted in (a), were subjected to IHC for OCN following Lac-Z staining. OCN-Lac-Z double positive cells are depicted as dark brown cells (indicated by arrow-heads); OCN single positive in orange; Lac-Z single positive (none in this section) as light blue.

B, calluses from mice that received either MSC-Lac Z or MSC^{IGF}-Lac Z transplant were analyzed at 7 days post-fracture by Lac-Z staining (a and b) and adjacent sections by Lac-Z staining followed by IHC for either pIRS1 (c and d) or OCN (e and f) or E11 (h and h) and ALP (j and k). Dotted squares in (a) indicate areas magnified respectively in (c), (e), (g) and (j); dotted squares in (b) the areas magnified in (d), (f), (h) and (k). Double positive (Lac-Z and IHC) cells are depicted as dark brown, IHC single positive in orange; Lac-Z single positive as light blue. See comments in the text. Bar, A, 500 μm (a, c); 100 μm (b,d); 50 μm(e, f). B, 100 μm (a, b), 50 μm (c,d,e,f,g,h,j,k).

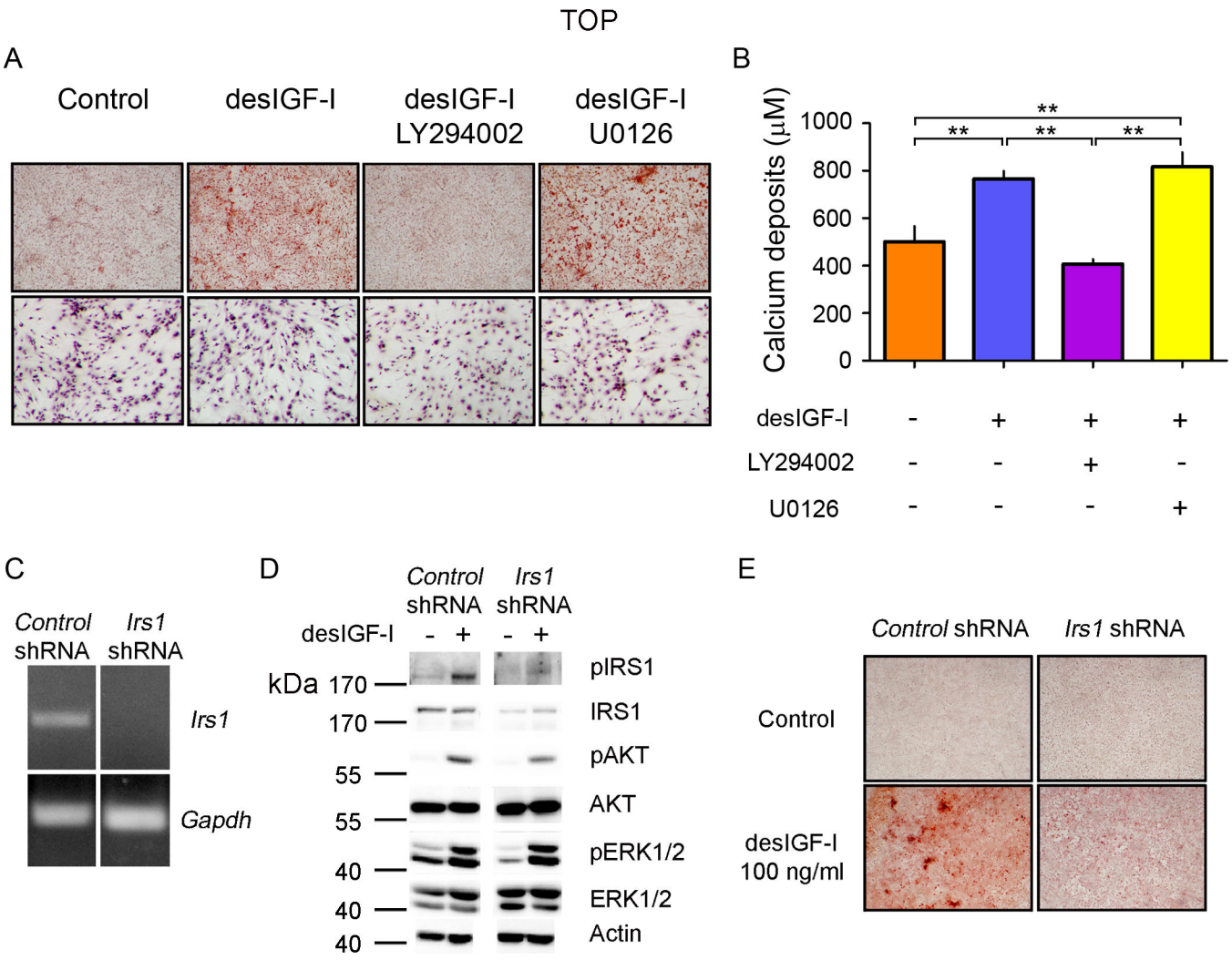

Figure 6.

IGF-I induces osteoblastic differentiation of MSC through the PI3K-AKT pathway. **A,** MSC cultures were grown to confluence and differentiated to osteoblasts in the presence or absence of either LY294002 (10 μM) or U0126 (5 μM) with or without desIGF-I (100 ng/ml) for 14 days. The presence of mineralization was detected by Alizarin Red staining, upper panels. The presence of attached cells was determined by Hematoxylin staining, lower panels. **B,** Calcium deposits were quantified in MSC cultured in osteogenic medium for 14 days. ANOVA p value=0.0001. **, p<0.01 by Bonferroni *ad hoc* test. n=3 for each group. **C,** MSC infected with retroviruses containing a scramble sequence (Control shRNA) or *Irs1* specific sequence (*Irs1* shRNA) were tested for the presence of Irs1 mRNA by RT-PCR. **D,** MSC infected with either with control shRNA or *Irs1* shRNA were treated with desIGF-I (100 ng/ml) for 10 minutes and protein extracts (10 μg) assayed for the presence of the indicated proteins or phosphorylated specific isoforms (p). **E,** Control and Irs1 silenced MSC cultures were induced to osteoblast differentiation in osteogenic medium with or without desIGF-I for 14 days (see Methods for more details). The presence of mineralization was detected by Alizarin Red staining.

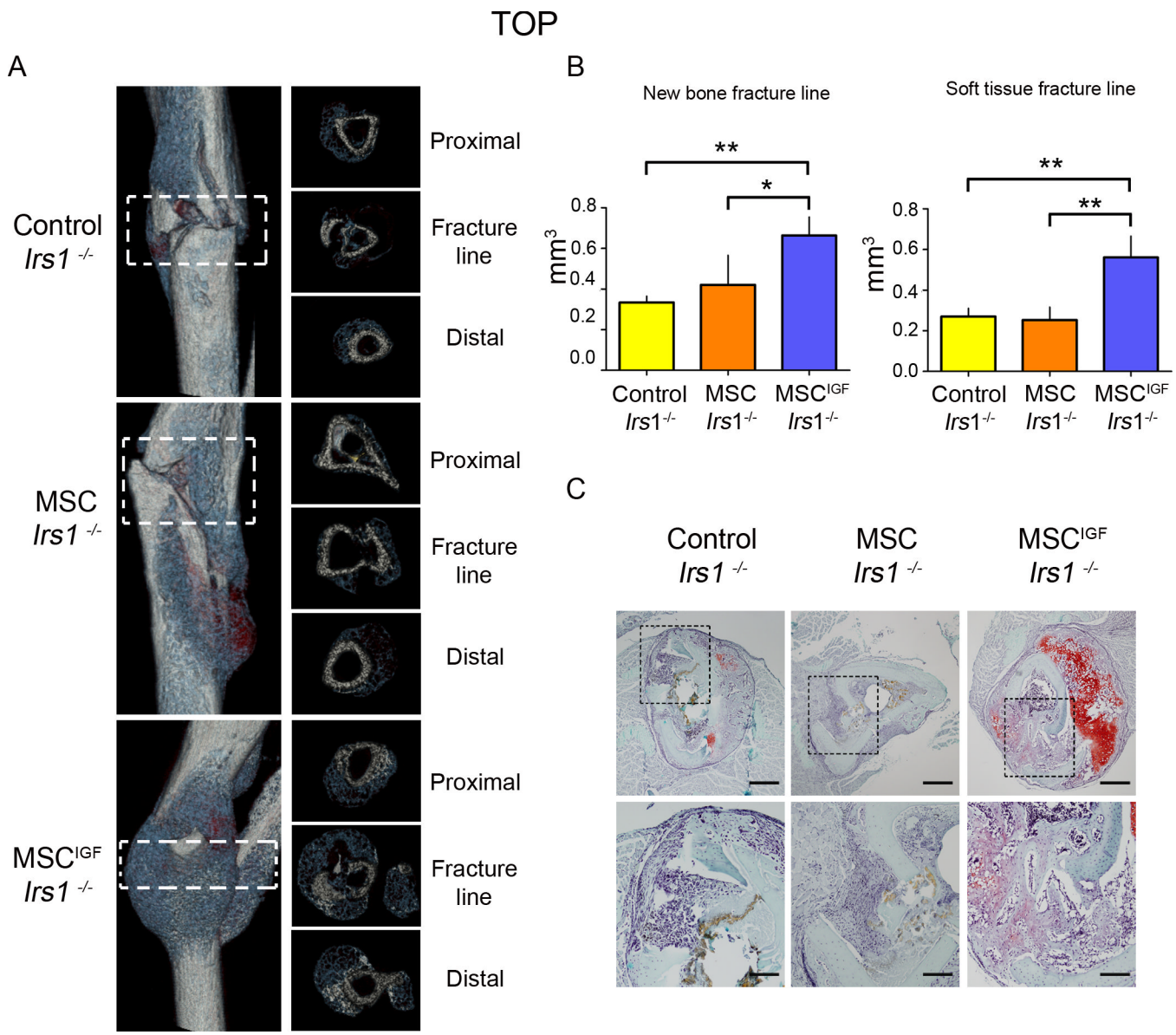

Figure 7.

MSC^{IGF} transplant improves the healing in a model of non-union tibia fracture (*Irs1*$^{-/-}$). **A,** Fourteen days after fracture, dissected tibias of *Irs1*$^{-/-}$ untransplanted (Control) or transplanted either with MSC or MSC^{IGF} were analyzed by μCT. Depicted are representative three dimensional reconstructions of the calluses from each group (left panel) and cross-sectional sections (right panel). **B,** New bone and soft tissue content at the fracture line were quantified using a μCT-histological-*in situ* based thresholding analysis (see Supplemental Methods). The fracture line was defined as the region comprised between the proximal to distal fracture borders, indicated by the dotted squares. Control; *Irs1*$^{-/-}$, n=3; MSC *Irs1*$^{-/-}$, n=4; MSC^{IGF} *Irs*$^{-/-}$, n=3. p values of one-way ANOVA analyses are respectively: new bone, p=0.0178; soft tissue, p=0.0018. *, p<0.05; **, p<0.01 by Bonferroni *ad hoc* test. **C,** Sequential cross-sections were stained for the presence of cartilage and bone tissue with Safranin O/Fast Green. Bar, 500 μm (upper panels) , 200 μm (lower panels).